Fuel 314 (2022) 122742

Contents lists available at ScienceDirect

Fuel

journal homepage: www.elsevier.com/locate/fuel

Coal and biomass combustion with CO_2 capture by CLOU process using a magnetic Fe-Mn-supported CuO oxygen carrier

Iñaki Adánez-Rubio *, Iván Samprón, María Teresa Izquierdo, Alberto Abad, Pilar Gayán, Juan Adánez

Instituto de Carboquímica (ICB-CSIC), Miguel Luesma Castán, 4, Zaragoza 50018, Spain

ARTICLE INFO

Keywords:
CO_2 capture
Chemical looping combustion
CLOU
Biomass
Coal

ABSTRACT

The Chemical Looping with Oxygen Uncoupling (CLOU) process is a derivative technology of the Chemical Looping Combustion (CLC) process for the combustion of both renewable and non-renewable solid fuels. The present work studies the combustion and CO_2 capture efficiency of burning coal or biomass using a single Cu-based oxygen carrier with magnetic properties as an oxygen carrier. The combustion of two different coals and three different biomasses was performed in a 1.5 kW_{th} CLOU continuously operated unit for 36 h. The magnetic properties of the oxygen carrier were also studied after combustion and its separation from the ashes. Complete combustion of the fuel to CO_2 and H_2O was achieved in all cases. For both coals, CO_2 capture efficiency increased with fuel reactor temperature, with both reaching values of 97% at 900 °C. The same increase was obtained with the biomasses. The highest CO_2 capture efficiency for a biomass was obtained with pine sawdust, which achieved a value of 93%, followed by almond shell (86%) and olive stone (80%) at 900 °C. Oxygen carrier reactivity remained constant after use in the continuous unit with one small increase in the attrition jet index (AJI) value. The used particles were found to still be as magnetic as the fresh particles, and the fines were also highly magnetic. Values higher than 99% were achieved with separation from the fines reached. It was therefore proven that the elutriated oxygen carrier from the plant was still magnetic and could be easily separated from the elutriated ash.

1. Introduction

The Chemical Looping with Oxygen Uncoupling (CLOU) process is a derivative technology of the Chemical Looping Combustion (CLC) process for the combustion of both renewable and non-renewable solid fuels [1]. CLOU technology, which takes advantage of the properties of certain metal oxides to generate gaseous oxygen at high temperatures, may be particularly suitable for solid fuels, such as coal and biomass. The oxygen generated by the oxygen carrier reacts directly with the solid fuel, with which it is mixed in the fuel reactor. Oxygen carriers for the CLOU process must be able to react with oxygen in the air reactor and then release this oxygen through decomposition in the fuel reactor [2,3]. Fig. 1 illustrates the CLOU process. The diagram includes a carbon stripper to enable the unburnt char to be recirculated to the fuel reactor.

Reviews reporting on the CLC process with solid fuels can be found elsewhere [2,4]. A number of different oxygen carriers have been developed for the CLOU process [2,4], such as Cu and Mn-based oxygen carriers [5–7], Cu-Mn mixed oxides [8,9], Ca-Mn perovskites [10–13] and other mixed oxides containing Ca, Ti, Mn, Mg and Fe [14–19].

Recently, CuO and Cu-Mn oxygen carriers have shown good performance for the combustion of coal and biomass, with a high oxygen transport capacity, high O_2 release rate, high CO_2 capture efficiencies and the complete combustion of gases in the fuel reactor [6–8,20–23]. Mn-based mixed oxides with a perovskite structure, such as $CaMnO_3$ doped with Mg or Ti, have shown good behaviour for the combustion of gaseous fuels [13,24,25], but present incomplete conversion of the gases during solid fuel combustion [14,15].

One of the problems arising from the use of solids fuels in CLC is the presence of ashes, which makes it necessary to drain material from the reactors, with the corresponding loss of oxygen carrier together with the ash. Moreover, the formation of fines generated by attrition, together with fine ash particles, increases oxygen carrier loss. Magnetic separation could be a useful method for separating and recovering lost oxygen carrier, enabling its reuse [2]. Therefore, the use of a single oxygen carrier for CLOU process with magnetic properties would improve the

* Corresponding author.
E-mail address: idanez@icb.csic.es (I. Adánez-Rubio).

https://doi.org/10.1016/j.fuel.2021.122742
Received 23 July 2021; Received in revised form 22 November 2021; Accepted 27 November 2021
Available online 10 December 2021

Nomenclature

Symbols

C_{AR}	Carbon exiting from the air reactor as CO_2 (kg/h)
C_{elut}	Carbon elutriated from the fuel reactor (kg/h)
C_{fix}	Fixed Carbon in the fuel(kg/h)
m_{5h}	Mass of fines collected from the attrition tester after 5 h (g)
m_s	Mass of sample loaded into the system attrition tester, nominally 50 g (g)
$\dot{m}_{SF}$	Mass flowrate of solid fuel fed into the fuel reactor (kg/h)
m^*_{FR}	Specific solids inventory (kg/MW_{th})
$\dot{m}_{oc}$	Solids circulation rate (kg/h)
R_{OC}	Oxygen transport capability (kg oxygen per kg of oxygen carrier)
X_{char}	Char conversion (-)

Greek letters

η_{CC}	CO_2 capture efficiency (-)
$\eta_{comb,FR}$	Combustion efficiency in the fuel reactor (-)
λ	Air excess ratio (-)
μ	Magnetic permeability (-)
ϕ	Oxygen carrier-to-fuel ratio (-)
ρ_{real}	Real density $\left(\frac{kg}{m^3}\right)$
χ_m	Magnetic volumetric susceptibility (m^3/kg)

Subscripts

outAR	Aire reactor outlet stream

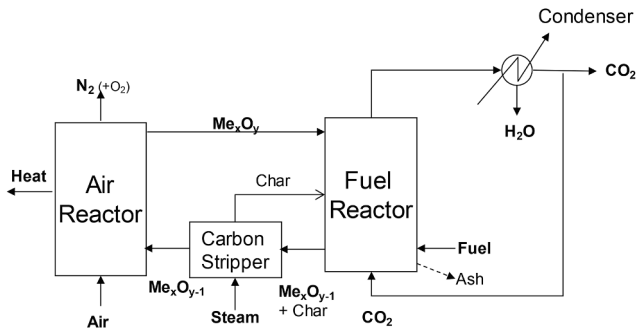

Fig. 1. CLOU unit scheme.

recovery and reuse of the material and reduce CLC operating costs when burning solid fuels with CO_2 capture.

With regard to oxygen carriers with magnetic properties, Mn-Fe-based oxygen carriers release O_2 by the CLOU mechanism through the decomposition of bixbyite [$(Mn_xFe_{1-x})_2O_3$] to spinel [$(Mn_xFe_{1-x})_3O_4$] [19,26]. However, their oxygen transport capacity is usually low, although the magnetic properties of some of these oxygen carriers have proven to remain constant after their use in continuous operation when burning solid and gas fuels [27]. The key factor for the use of oxygen carriers of this type is that they maintain their magnetic properties after use in a continuous unit. It is therefore necessary to make this material inert for reaction while keeping its magnetic properties. In this regard, Perez-Vega developed a magnetic material that was inert for CLC and CLOU reactions but highly magnetic for use as a support for CLOU materials [28,29].

In a previous work, two Cu-based oxygen carriers supported on a Mn-Fe mixed oxide were developed for the CLOU process [28]. They offered high reactivity, a high oxygen transport capacity and high and stable magnetic permeability after use in a batch fluidized bed reactor [30]. One of these was selected for the present work in order to analyse its performance for the CLOU process when burning coals of different rank and different biomasses in a 1.5 kW_{th} continuous unit.

The aim of the present work is to analyse the performance of a Cu-based oxygen carrier with magnetic properties for the combustion of five renewable and non-renewable fuels in a 1.5 kW_{th} CLOU continuous unit. The study was made of the effects of fuel type, fuel reactor temperature and oxygen excess in the air reactor on combustion and CO_2 capture efficiencies, and char conversion. The effect of continuous operation on the reactivity and magnetic properties of the oxygen carrier, and the ability of the oxygen carrier fines to be separated from both the elutriated ashes and bed material were also studied.

2. Experimental

2.1. Oxygen carrier

A Cu-based oxygen carrier developed at ICB-CSIC [30] was prepared in a spouted fluidized bed system (Glatt W51530 + OPP1) by spray granulation. As a support material, a magnetic Fe-Mn mixed oxide was prepared according to a patented method [29]. The oxygen carrier was prepared using Mn_3O_4 (Elkem), Fe_2O_3 (Acros chemicals) and CuO (Panreac, PRS) as raw materials. The amount of CuO in the particles was of 30 wt% and the molar ratio of manganese to iron was 1:1. The Fe-Mn magnetic support was previously prepared to preserve its magnetic properties. After granulation of the CuO powder together with the magnetic support, the particles were calcined for 4 h at 1100 °C. The main properties of the oxygen carrier are shown in Table 1. The oxygen carrier particle size used was + 0.1–0.3 mm. The name given to the oxygen carrier is Cu30MnFe_Mag.

2.2. Oxygen carrier characterization

The chemical and physical characteristics of the oxygen carrier were determined by different methods. Crushing strength, jet attrition test index, particle size, pore volume, density, specific surface area and crystalline phases were also analysed. As was observed in a previous study by Adánez-Rubio et al. [30], the main phases of the developed oxygen carrier were Fe_3O_4, Fe_5CuO_8 and $Cu_{0.5}Mn_{0.5}FeO_4$. Moreover, CuO, $CuFeO_2$ and $MnFe_2O_4$ were observed as minor phases. The oxygen transport capacity for CLOU (R_{OC}) was determined by weight loss in N_2 atmosphere at 950 °C in a thermogravimetric analyser. The R_{OC} value was shown to be higher than the theoretical value only when the CuO functioned as the active phase (2.0 vs 1.5 wt%), see Table 1. Therefore, the Mn and the Fe not only gave the particles magnetic properties but also improved their oxygen transport capacity.

The crushing strength of the carrier particles was determined in a Shimpo FGN-5X crushing strength apparatus as an average value of 20 measurements, with particles sized + 0.1–0.3 mm. The ATTRI-AS three-hole air jet attrition testing instrument (MaTec. Materials Technologies Snc) configured according to the ASTM-D-5757 standard [31] was used to determine low-temperature attrition resistance.

Table 1
Properties of the Cu30MnFe_Mag oxygen carrier used in this work: fresh and used after 63 h of continuous operation.

	Fresh	Used 63 h
Oxygen transport capacity for CLOU, R_{OC} (wt%)	2.0	2.0
Crushing strength (N)	2.2	2.1
Skeletal density of particles (kg/m^3)	5125	5138
AJI (%)	0.3	3.4
Porosity (%)	51.6	57.4
Specific surface area, BET (m^2/g)	< 0.5	< 0.5

2.3. Solid fuels

Two coals and three biomasses were used for the CLOU experiments with the Cu30MnFe_Mag oxygen carrier. A medium-volatile bituminous coal (MVB) from Taldinski (Russia) and a subbituminous coal (SB) from Mina Invierno (Chile) were used for the purpose of covering different ranks of coal. Pine (*Pinus sylvestris*) sawdust, almond (*Prunus dulcis*) shells and olive (*Olea europaea*) stones were the biomasses used due to their general availability and their high annual production [32,33], respectively. The proximate and ultimate analyses of the coals and biomasses are shown in Tables 2 and 3, respectively. Particle size was + 0.1–0.3 for coals and + 0.5–2 mm for biomasses.

2.4. Experimental set-up

Fig. 2 provides a schematic view of the 1.5 kW_{th} CLOU continuous unit. The set-up basically comprised two interconnected fluidized bed reactors –the air and fuel reactors – joined by a loop seal, a riser for solids transport from the air reactor to the fuel reactor, a cyclone and a solids valve to control the solids circulation flow rate in the system. A diverting solids valve located below the cyclone allowed for measurement of the solid circulation flow rate at any time. Therefore, this design allowed the solids circulation flow rate between both reactors to be controlled and measured. A detailed description of the continuous unit can be found elsewhere [20].

N_2 was used as the fluidizing gas in the fuel reactor for better control of the process results. Recirculated CO_2 will be used in industrial units. The temperature of the fuel reactor was varied within the range of 750–900 °C and the gas flow was 300 Nl/h of N_2, corresponding to a gas velocity of 0.15 m/s of in the fuel reactor under operating conditions. The temperature in the air reactor was fixed at 850 °C and fluidized with a flow of 2600 Nl/h of air or air/N_2 mixtures to regenerate the oxygen carrier. The loop-seal was fluidized with a N_2 flow of 90 Nl/h to prevent mixing between the fuel and air reactor gas flows. The fuel was fed in by a double screw feeder just above the distributor plate in the fuel reactor to maximize the residence time of the volatile matter and char in contact with the oxygen carrier inside this reactor. In addition, in order to avoid the reverse of gas flow from the fuel reactor through the solid feed system, a N_2 flow of 18 Nl/h was fed at the entry to the screw feeders.

The inventory of oxygen carrier in the continuous unit was 3.4 kg, while the fuel reactor inventory was about 1 kg. CO, CO_2, H_2, CH_4 and O_2 were continuously analysed at the fuel reactor outlet:, while CO, CO_2 and O_2 were analysed at the air reactor outlet. Non-dispersive infrared (NDIR) analysers (Siemens Ultramat 23) were used to analyse the CO_2, CO and CH_4. For were used paramagnetic analysers (Siemens Ultramat 23 and Oxymat 6) were used for the O_2, and a thermal conductivity detector (Siemens Calomat 6) was used to analyse the H_2.

Table 2
Properties of the coals used in this work.

	Medium-volatile bituminous coal Taldinski (Russia)	Subbituminous coal Mina Invierno (Chile)
Proximate Analysis (wt%)		
Moisture	5.8	14.2
Volatile matter	32.0	34.6
Fixed carbon	52.1	35.9
Ash	10.1	15.3
Ultimate Analysis (wt%)		
C	65.8	52.4
H	4.6	5.24
N	2.0	0.77
S	0.5	0.2
O*	11.3	11.9
LHV (kJ/kg)	26,600	18,900

*By difference

Table 3
Properties of the biomass used in this work.

	Pine sawdust	Almond shell	Olive stone
Proximate Analysis (wt%)			
Moisture	4.2	2.3	9.4
Volatile matter	81.0	76.6	72.5
Fixed carbon	14.4	20.0	17.3
Ash	0.4	1.1	0.8
Ultimate Analysis (wt%)			
C	51.3	50.2	46.5
H	6.0	5.7	4.8
N	0.3	0.2	0.2
S	0.0	0.0	0.0
O*	37.8	40.5	38.3
LHV (kJ/kg)	19,158	18,071	17,807

*By difference

2.5. Experimental planning

The experimental work analysed the effect of temperature on the combustion performance of two coals and three different biomasses. The effect of the oxygen excess on the performance of pine sawdust combustion was also studied. The main operating variables used in the coal and biomass combustion are summarized in Table 4. The same batch of oxygen carrier particles was used for 36 h of combustion and 63 h of hot fluidization. The fuel feeding rate varied between 110 and 170 g/h, corresponding to power inputs of between 680 and 840 W_{th}. The oxygen carrier circulation rate was modified within the 14–22 kg/h range, corresponding to oxygen carrier-to-fuel ratio values of between 2.3 and 3.

3. Data evaluation

The attrition jet index value (AJI) was calculated by considering the weight of the fine particles recovered in the filter after 5 h of testing using this equation:

$$\mathrm{AJI} = \frac{m_{5h}}{m_s} \tag{1}$$

Magnetic permeability, μ (-), was calculated as follows:

$$\mu(-) = 1 + \chi_m \left(\frac{m^3}{kg}\right) \cdot \rho_{real} \left(\frac{kg}{m^3}\right) \tag{2}$$

where χ_m (m^3/kg) is the magnetic volumetric susceptibility of the oxygen carrier as measured using the MS2G magnetic susceptibility meter (single frequency sensor) connected to an MS3 magnetic susceptibility meter (Bartington Instruments). The magnetic susceptibility readings given by the sensor were relative to air, with the meter being reset to zero for this purpose. The value reported for each oxygen carrier was the average value of 3 consecutive measurements. ρ_{real} is the density of the oxygen carriers (kg/$m^{3)}$. Density was measured with a Micromeritics AccuPyc II 1340 helium pycnometer.

The oxygen carrier-to-fuel ratio (ϕ) was defined by the following equation [8]:

$$\phi = \frac{\text{Oxygen supply by the oxygen carrier}}{\text{Oxygen demanded by the fuel for full combustion}} \tag{3}$$

The air excess ratio, λ, was defined by equation (4), and the values for the experimental work were always greater than 1.

$$\lambda = \frac{\textit{Oxygen fed to the air reactor}}{\textit{Oxygen demanded by the fuel for full combustion}} \tag{4}$$

Combustion and CO_2 capture efficiencies were calculated in order to study the performance of the CLOU process. The calculations were made with every analysed gas molar flow, F_i, calculated from the measured gas concentration. Combustion efficiency in the fuel reactor ($\eta_{Comb,FR}$) was defined as the fraction of oxygen demanded by the volatile matter

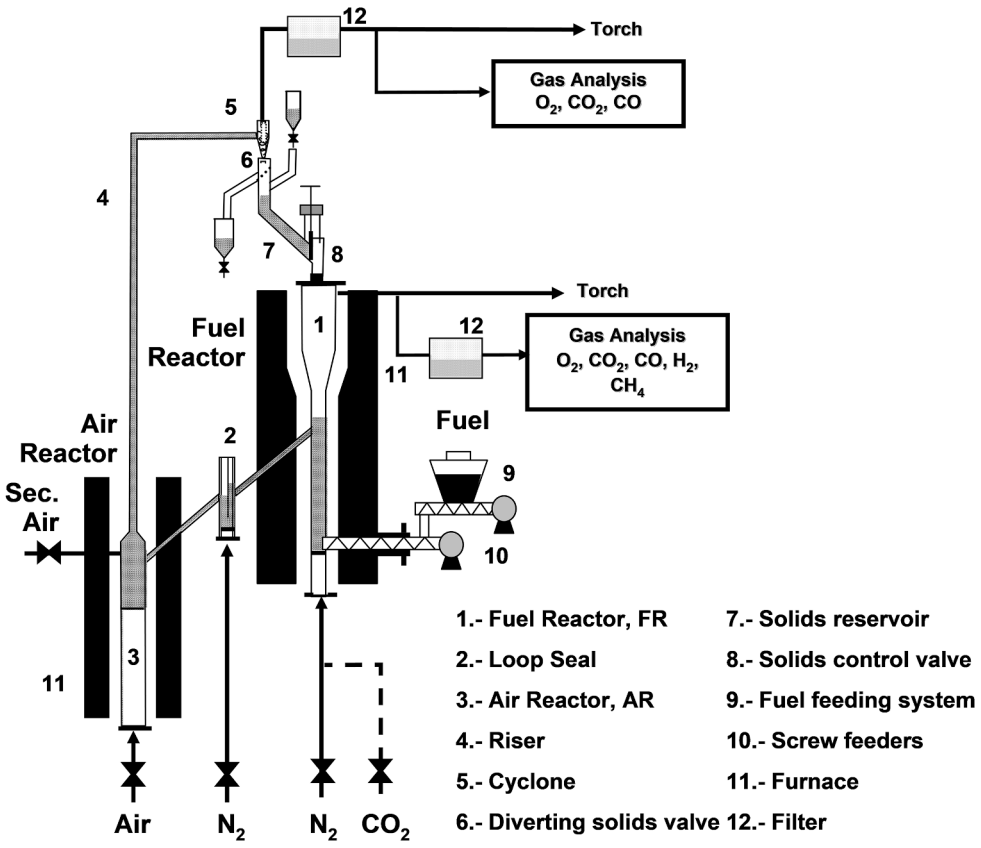

Fig. 2. Schematic view of the ICB-CSIC-s1 unit.

and converted char inside the fuel reactor that was supplied by the oxygen carrier and calculated as follows:

$$\eta_{Comb,FR} = 1 - \frac{oxygen\ demanded\ by\ unburnt\ gases}{oxygen\ demanded\ by\ solid\ fuel\ converted\ in\ fuel\ reactor} \quad (5)$$

CO_2 combustion efficiency was relative to the amount of carbon initially present in the fuel that exited the fuel reactor outlet as CO_2.

$$\eta_{CC} = \frac{CO_2\ in\ gases\ from\ fuel\ reactor}{carbon\ in\ gases\ from\ fuel\ and\ air\ reactors} \quad (6)$$

CO_2 capture efficiency depended on the amount of unburnt char transferred from the fuel reactor to the air reactor. It was therefore dependent on rate of char conversion. Char conversion was calculated by taking into account the amount of char burnt in the fuel reactor and char fed to the fuel reactor as fixed carbon:

$$X_{char} = \frac{C_{fix} - C_{outAR} - C_{elut}}{C_{fix} - C_{elut}} \quad (7)$$

4. Results and discussion

4.1. Coal combustion and CO_2 capture efficiency

Coal combustion was carried out for 14 h by burning two different coals at fuel reactor temperatures ranging between 750 and 900 °C. It was observed that during the heating period from ambient temperature, the material was able to generate O_2 gas at fuel reactor operating temperatures starting at 750 °C. Once the fuel feeding commenced, no gaseous oxygen was detected in the fuel reactor flue gas, as can be seen in Fig. 3.

Fig. 4 shows combustion and CO_2 capture efficiencies, as well as the char conversion obtained during the combustion of the MBV coal and SB coals. In all cases, even at the lowest temperature tested (750 °C), a combustion efficiency higher than 99% was achieved for MBV coal, see Fig. 4a. Thus, the fuel reactor gases were fully oxidized and no oxygen polishing step [34] was required to complete the combustion. CO_2 capture efficiency increased with increasing fuel reactor temperature from 73% at 750 °C to 97% at 900 °C. The high CO_2 capture efficiencies achieved at these fuel reactor temperatures lower than 900 °C are of note. The increase in CO_2 capture efficiency was attributed to the increase in char conversion in the fuel reactor. As the conversion of char inside the fuel reactor increased, less unburnt char was transported to the air reactor, increasing CO_2 capture efficiency. Carbon balances performed with MVB coal showed a high elutriation of unburnt char, equivalent to 40% of the carbon fed into the system. Thus, the less carbon transferred to the air reactor, similar to a reduction in the coal fed into the system, the higher the CO_2 capture. Moreover, the low reactivity of this char did not allow the combustion of comminute small particles before being entrained from the fuel reactor. This was a consequence of the design of the unit, which did not provide for recirculation of the elutriated char material. This problem should be solved in an industrial unit with one circulating fuel reactor and a carbon stripper because the elutriated char will largely be recirculated to the fuel reactor for burning.

The effect of coal rank was also studied. For this purpose, SB coal with a power of 840 W_{th} was fed to the unit. Fig. 4b shows the combustion and CO_2 capture efficiencies and the char conversion found. For both coals, a combustion efficiency of over 99.9% was observed throughout the temperature range studied. On the other hand, it was observed that, as in the case of MBV coal, as the fuel reactor temperature increased, CO_2 capture efficiency and char conversion increased. Unlike MBV coal, where there was a large amount of unconverted char elutriated, in the case of the SB coal, the carbon balance closed with an error lower than 5%, and therefore the amount of elutriated char was minimum. This fact that a lower amount of carbon was elutriated from the fuel reactor was behind the higher char conversion values for SB coal in

Table 4
Main data for experimental tests in the 1.5 kW_{th} CLOU unit with coal and biomass.

Fuel	Test	$\dot{m}_{oc}$ (kg/h)	$\dot{m}_{SF}$ (g/h)	Power (W_{th})	T_{FR} (°C)	ϕ	λ	m^*_{FR} (kg/MW_{th})
MVB	R01	14	110	800	**750**	2.5	3.3	910
MVB	R02	14	110	800	**800**	2.5	3.3	910
MVB	R03	14	110	800	**850**	2.5	3.3	910
MVB	R04	14	110	800	**900**	2.5	3.3	910
SB	C01	16	160	840	**750**	2.9	3.0	990
SB	C02	16	160	840	**800**	2.9	3.0	990
SB	C03	16	160	840	**850**	2.9	3.0	990
SB	C04	16	160	840	**900**	2.9	3.3	990
Pine sawdust	P01	18	140	745	**750**	2.3	4.0	1100
Pine sawdust	P02	18	140	745	**800**	2.3	4.0	1100
Pine sawdust	P03	18	140	745	**850**	2.3	4.0	1100
Pine sawdust	P04	18	140	745	**900**	2.3	4.0	1100
Pine sawdust	P05	22	145	775	850	2.6	**3.8**	1075
Pine sawdust	P06	22	145	775	850	2.6	**1.8**	1075
Pine sawdust	P07	22	145	775	850	2.6	**1.4**	1075
Pine sawdust	P08	22	145	775	850	2.6	**1.2**	1075
Almond shells	A01	18	170	785	**750**	2.5	4.1	1080
Almond shells	A02	18	170	785	**800**	2.5	4.1	1080
Almond shells	A03	18	170	785	**850**	2.5	4.1	1080
Almond shells	A04	18	170	785	**900**	2.5	4.1	1080
Olive stones	O01	21	135	680	**750**	3	4.3	1200
Olive stones	O02	21	135	680	**800**	3	4.3	1200
Olive stones	O03	21	135	680	**850**	3	4.3	1200
Olive stones	O04	21	135	680	**900**	3	4.3	1200

The bold values represent the parameter that has been studied and varied in each experimental point.

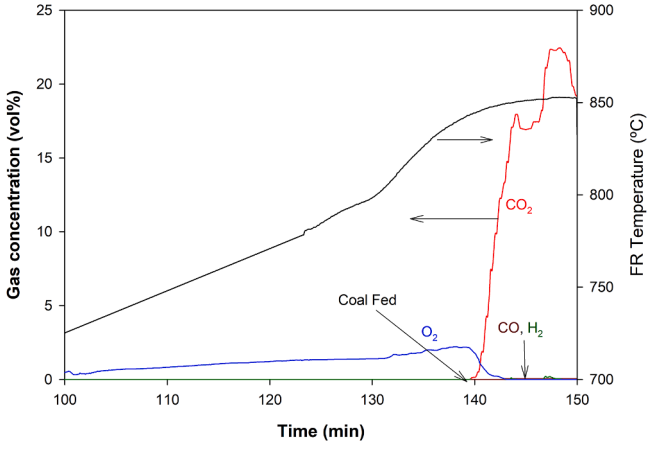

Fig. 3. Evolution of the gas composition in the fuel reactor during the heating up and commencement of coal feeding. Experimental tests R03. T_{AR} = 850 °C; ϕ = 2.5; Power = 800 W_{th}.

all the fuel reactor temperature range studied. However, the CO_2 capture efficiency with the MBV coal was higher than that achieved with SB coal with fuel reactor temperatures lower than 900 °C due to the unburnt char being elutriated instead of being transferred to the air reactor, therefore magnifying its CO_2 capture efficiency. If all the elutriated char from the MBV coal had been transferred to the air reactor, its CO_2 capture efficiency would have decreased, reaching a maximum of 82% at 900 °C instead of 97%.

4.2. Biomass combustion and CO_2 capture efficiency

Biomass combustion tests were carried out for 22 h with three different types of biomass: pine sawdust, almond shells and olive stones. In all cases, the biomass was fed with a thermal power input of between 680 and 780 W_{th}.

Fig. 5 shows the CO_2 capture efficiency (Fig. 5a) and char conversion (Fig. 5b) achieved with the different biomasses used. Combustion efficiencies higher than 99.9 % were obtained with all the biomasses, even at the lowest temperature of 750 °C, , with 100% achieved at 900 °C in all cases. CO_2 capture efficiency increased with increasing temperature due to the increase in char conversion in the fuel reactor (see Fig. 5b). Higher values at temperatures lower than 900 °C were found with respect to coal combustion due to the higher combustion reactivity of the biomass char compared to that of the coal char. This can be also attributed to the high volatile content in biomass, which is more easily burnt. The highest CO_2 capture efficiency was achieved with pine biomass, reaching a value of 93% at 900 °C. The highest CO_2 capture efficiencies were also found with this biomass when a Cu-Mn mixed oxide was used as the oxygen carrier [23]. As observed in previous works, this is the most reactive biomass and the one with which the best CO_2 capture efficiency results with biomasses were obtained with the use of a Cu-Mn mixed oxide [23].

Lower CO_2 capture efficiencies were obtained both for almond shells and olive stones due to the lower reactivity of the char generated, with 86% and 80% CO_2 capture efficiencies at 900 °C, respectively. It can be concluded that to achieve high CO_2 capture efficiencies above 95% with biomass, it is necessary to operate at temperatures higher than 900 °C in the fuel reactor. For all the biomasses, the carbon balance closed with errors lower than 5%, and therefore the amount of elutriated char was minimal.

Furthermore, the effect of air excess ratio (λ) was analysed during the combustion of the pine biomass. The temperature was kept fixed at 850 °C in both the fuel and air reactors. Fig. 6 plots the CO_2 capture efficiencies found as a function of λ. For values between 1.2 and 4, complete combustion was observed in all cases. In addition, CO_2 capture efficiency remained stable at between 91 and 92%. Therefore, the excess of oxygen in combustion did not significantly affect CO_2 capture efficiency.

4.3. Oxygen carrier characterization

After the combustion experiments carried out in the 1.5 kW_{th} continuous unit, the magnetic permeability was measured for the particles extracted from the fuel and air reactors, and the elutriated particles containing fines that were recovered by the cyclones. Moreover, the reactivity, AJI, crushing strength and magnetism of both fresh and used particles were analysed. Fines particles of a size lower than 45 μm were sieved from elutriated particles recovered by the cyclones.

With regard to magnetic permeability (μ), Table 5 shows that the particles inside the continuous unit were still as magnetic as the fresh ones. The fines were also highly magnetic. A small commercial magnet was used to verify the separation of the oxygen carrier from the ashes. The fines were separated from ashes with a separation efficiency of 99 wt%. With regard to the material extracted from both the fuel and air reactors, oxygen carrier recovery of 98% and 98.5%, respectively, could be verified. The oxygen carrier extracted from the unit was

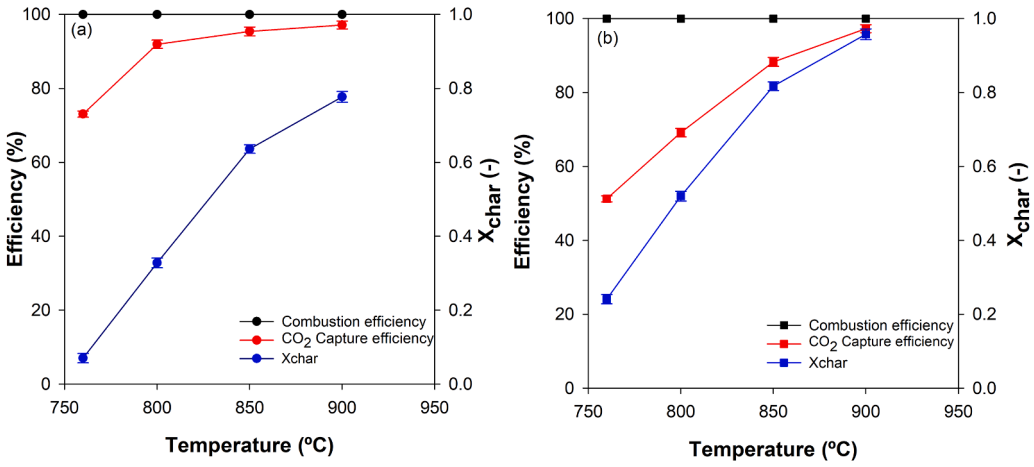

Fig. 4. Effect of fuel reactor temperature on combustion and CO_2 capture efficiencies and char conversion when burning fuels: a) MBV coal; and b) SB coal. T_{AR} = 850 °C; ϕ = 2.2–2.9; Power = 800–840 wt

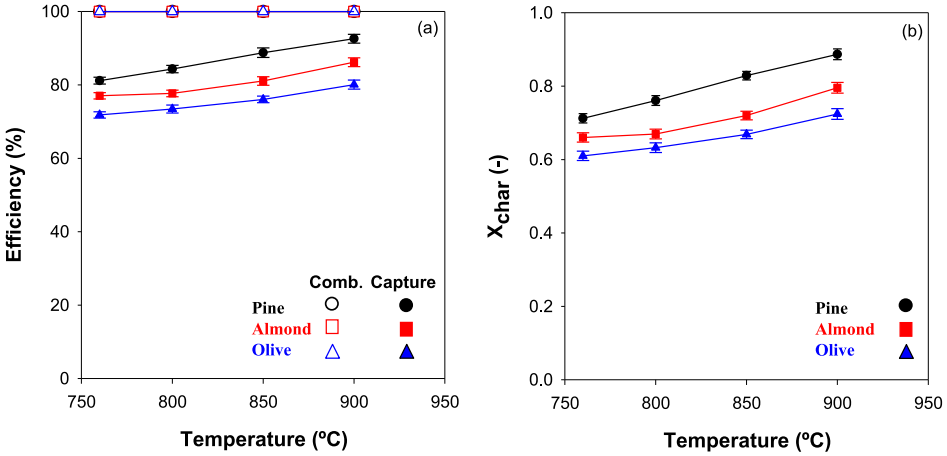

Fig. 5. Effect of fuel reactor temperature on: (a) CO_2 capture efficiency and (b) char conversion when burning three kinds of biomass: pine sawdust, almond shells and olive stones. T_{AR} = 850; ϕ = 2–3; Power = 680–780 W_{th}.

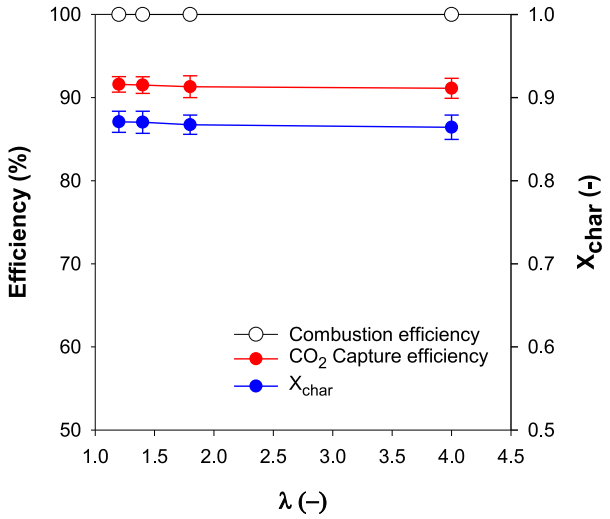

Fig. 6. Effect of air excess ratio in the air reactor during the combustion of pine sawdust on the CO_2 capture efficiency and char conversion. T_{FR} = 850; T_{AR} = 850; ϕ = 2.5; Power = 750 W_{th}.

Table 5
Magnetic permeability and oxygen carrier recovery for fresh and used particles extracted from the continuous unit, and fines.

	Fresh	Used 36 h (AR)	Fines
μ (-)	3.4	3.2	4.1
	FR	AR	Fines (<45 μm)
OC recovery	98%	98.5%	99%

demonstrated to still be magnetic and could easily be separated from the elutriated coal ash.

The reactivity of the oxygen carrier remained constant after 36 h of combustion, even with the presence of different ashes in the fuel reactor, see Fig. 7.

Table 1 shows that crushing strength remained fairly stable, although the attrition jet index (AJI) increased from 0.6% to 3.4% after 36 h of combustion; however, it was still below the 5% considered acceptable for FCC catalysts, which means that the oxygen carrier showed good mechanical stability with operation time.

4.4. Discussion

The results obtained with the present oxygen carrier can be compared with previous Cu and CuMn-based oxygen carriers. As regards coal combustion, similar results were obtained with a Cu-Mn mixed

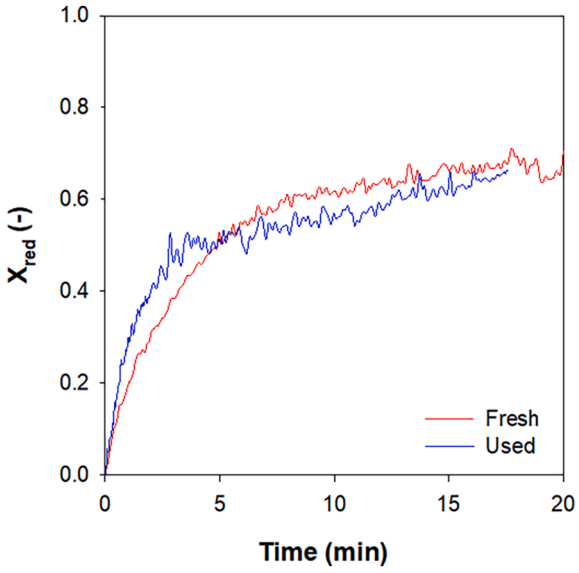

Fig. 7. Oxygen uncoupling conversion obtained in the thermogravimetric analyser with fresh and used oxygen carrier after 36 h of combustion in the 1.5 kW_{th} continuous unit. Reduction: N_2, T = 950 °C.

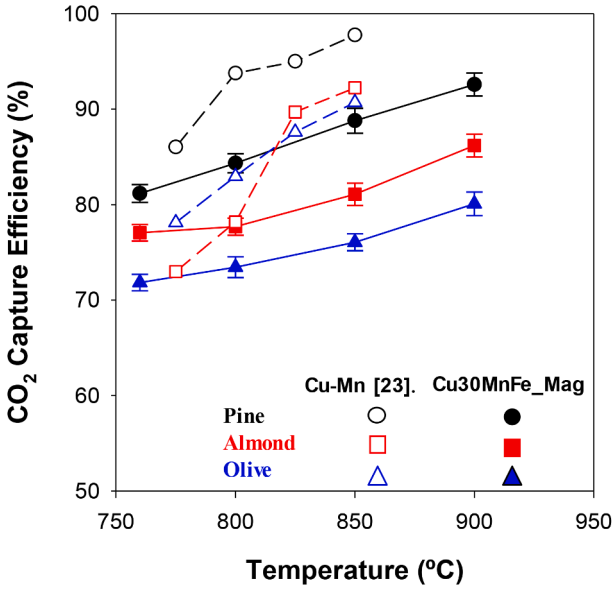

Fig. 8. Effect of fuel reactor temperature on CO_2 capture efficiency as a function of the oxygen carrier used: Cu-Mn mixed oxide [23] and Cu30MnFe_Mag.

oxide in a 1.5 kW_{th} continuous unit burning the same coals [8,21]. However, when using a Cu-based oxygen carrier, it was necessary to operate at a temperature of at least 925 °C in the fuel reactor to reach similar CO_2 capture efficiencies [6,20]. Adánez-Rubio et al. found CO_2 capture values of around 94–98% using MVB coal and bituminous "El Cerrejón" Bituminous coal, respectively, when operating at a temperature range of 900–925 °C using CuO on $MgAl_2O_4$ as oxygen carrier with a higher CuO content (60 wt%). Note that gaseous oxygen concentration released at equilibrium ranged between 0.1 vol% at 800 °C and 1.5 vol% at 900 °C for CuO, with negligible concentrations found at temperatures lower than 800 °C. Thus, the high CO_2 capture found at low temperatures could be attributed to the O_2 released by the different mixed oxides generated that contained Fe and Mn, alone or with Cu, present in the material used as support. The oxygen carrier in this case released O_2 at lower temperatures than CuO, although the mixed oxide had been inertized during preparation [27,28]. Thus, the presence of Mn-Fe mixed oxides, already having a small CLOU effect by itself, improves the CO_2 capture efficiency performance of this Cu-based oxygen carrier when burning coal.

Where the biomasses were used as fuel, the results obtained with the Cu30MnFe_Mag improved the values obtained with a single-oxide, 60% CuO on $MgAl_2O_4$ oxygen carrier burning pine sawdust, which needed a temperature of at least 900 °C inside the fuel reactor to achieve complete combustion there, with a similar CO_2 capture efficiency achieved at this temperature [7]. However, better results were found using a Cu-Mn mixed oxide as oxygen carrier in the interval of fuel reactor temperatures studied for pine sawdust combustion, and slightly better with almond and olive stones [23], as can be seen in Fig. 8.

The combustion efficiencies found for the coals and biomasses used indicated that very high and similar values (greater than 99.9 %) were reached regardless of fuel reactivity, showing the very high reactivity of the volatile matter with the gaseous oxygen released by the oxygen carrier. Note the important differences in the volatile matter content in the biomasses (75–80 %) and in the coals (about 35%).

The differences found in CO_2 capture efficiencies are related to the amount of char transferred to the air reactor for burning, reducing the capture efficiency. Coal char conversion showed a single strong increase with temperature (see Fig. 3); however, in the case of the biomasses, char conversion was always high, although dependence on temperature was less important. These differences must be attributed to differences in char reactivities. It is well known that biomass char has a higher reactivity than coal char, although subbituminous coals are highly reactive. However, it is necessary to also consider that particle size distribution was much higher in the biomasses (+0.5–2 mm) than in the coals used (+0.1–0.3 mm), which obviously reduces their char conversion rates.

Therefore, the developed oxygen carrier shows a good performance for the combustion of different types of fuels and good mechanical stability. It also retained its magnetic properties to make it easily separable from the elutriated ashes.

5. Conclusions

The combustion of two different coals and three biomasses in a 1.5 kW_{th} CLOU continuous unit of for 36 h was studied using a Cu-based oxygen carrier with magnetic properties. the effect of the process on the magnetic properties of the oxygen carrier after the combustion of different fuels and their separation from the ashes was also investigated.

The CO_2 capture efficiency for both coals increased with fuel reactor temperature, achieving values of 97% at 900 °C. The same behaviour was observed with the biomasses, although lower CO_2 capture efficiencies were always found with respect to the highly reactive coal used. The highest CO_2 capture efficiency for a biomass was obtained with pine sawdust, with a value of 93% reached at 900 °C. Lower CO_2 capture efficiencies were found with almond shells and olive stones due to the lower reactivity of the char generated, with 86% and 80% CO_2 capture efficiencies achieved, respectively, at 900 °C. Thus, in order to achieve CO_2 capture efficiencies above 95% with biomass, it is necessary to exceed 900 °C in the fuel reactor.

The effect of excess of oxygen on the combustion of the pine biomass was also analysed. With air excess ratio values between 1.2 and 4, CO_2 capture efficiency remained stable above 91%. Therefore, excess oxygen did not affect CO_2 capture efficiency.

The reactivity of the oxygen carrier was found to remain constant after 36 h of combustion, with a small increase in the AJI value of between 0.6% and 3.4%, but still below the 5% limit value. The used particles were still as magnetic as the fresh ones. The recovered fines were also highly magnetic. Separation of the oxygen carrier from recovered ashes and from both fuel and air reactor solids shows efficiencies higher than 98%. It was therefore proven that the elutriated oxygen carrier from the plant was still magnetic and could be separated easily from the elutriated coal ash.

CRediT authorship contribution statement

Iñaki Adánez-Rubio: Investigation, Methodology, Data curation, Validation, Writing – original draft, Writing – review & editing. **Iván Samprón:** Investigation, Data curation. **María Teresa Izquierdo:** Data curation, Writing – review & editing. **Alberto Abad:** Resources, Funding acquisition, Writing – review & editing. **Pilar Gayán:** Resources, Funding acquisition, Writing – review & editing. **Juan Adánez:** Conceptualization, Resources, Supervision, Funding acquisition, Writing – review & editing.

Declaration of Competing Interest

The authors declare that they have no known competing financial interests or personal relationships that could have appeared to influence the work reported in this paper.

Acknowledgement

The work presented in this article was supported by the SWINELOOP project (Grant PID2019-106441RB-I00 funded by MCIN/AEI/ 10.13039/501100011033) and the Spanish Research Council (CSIC) through the Intramural Project (201980E043). I. Adánez-Rubio acknowledges for "Juan de la Cierva" Program (Grant IJC2019-038987-I funded by MCIN/AEI/10.13039/501100011033). I. Samprón acknowledges for the pre-doctoral fellowship (Grant PRE-086217 funded by MCIN/AEI/ 10.13039/501100011033 and by "ESF Investing in your future").

Bibliography

[1] Adanez J, Abad A, Garcia-Labiano F, Gayan P, de Diego L. Progress in Chemical-Looping Combustion and Reforming technologies. Prog. Energy Combust. Sci. 2012;38(2):215–82.
[2] Adánez J, Abad A, Mendiara T, Gayán P, de Diego LF, García-Labiano F. Chemical looping combustion of solid fuels. Prog. Energy Combust. Sci. 2018;65:6–66.
[3] Mattisson T, Lyngfelt A, Leion H. Chemical-looping with oxygen uncoupling for combustion of solid fuels. Int. J. Greenh. Gas Control 2009;3(1):11–9.
[4] Lyngfelt A, Brink A, Langørgen Ø, Mattisson T, Rydén M, Linderholm C. 11,000 h of chemical-looping combustion operation—Where are we and where do we want to go? Int. J. Greenh. Gas Control 2019;88:38–56.
[5] Imtiaz Q, Hosseini D, Müller CR. Review of Oxygen Carriers for Chemical Looping with Oxygen Uncoupling (CLOU): Thermodynamics, Material Development, and Synthesis. Energy Technol. 2013;1(11):633–47.
[6] Adánez-Rubio I, Abad A, Gayán P, de Diego LF, García-Labiano F, Adánez J. Performance of CLOU process in the combustion of different types of coal with CO_2 capture. Int. J. Greenh. Gas Control 2013;12:430–40.
[7] Adánez-Rubio I, Abad A, Gayán P, de Diego LF, García-Labiano F, Adánez J. Biomass combustion with CO_2 capture by chemical looping with oxygen uncoupling (CLOU). Fuel Process. Technol. 2014;124:104–14.
[8] Adánez-Rubio I, Abad A, Gayán P, de Diego LF, Adánez J. CLOU process performance with a Cu-Mn oxygen carrier in the combustion of different types of coal with CO_2 capture. Fuel 2018;212:605–12.
[9] Adánez-Rubio I, Abad A, Gayán P, Adánez I, de Diego LF, García-Labiano F, et al. Use of Hopcalite-Derived Cu-Mn Mixed Oxide as Oxygen Carrier for Chemical Looping with Oxygen Uncoupling Process. Energy Fuels 2016;30(7):5953–63.
[10] Schmitz M, Linderholm CJ. Performance of calcium manganate as oxygen carrier in chemical looping combustion of biochar in a 10 kW pilot. Appl. Energy 2016;169:729–37.
[11] Moldenhauer P, Hallberg P, Biermann M, Snijkers F, Albertsen K, Mattisson T, et al. Oxygen-Carrier Development of Calcium Manganite-Based Materials with Perovskite Structure for Chemical-Looping Combustion of Methane. Energy Technol. 2020;8(6):2000069. https://doi.org/10.1002/ente.202000069.
[12] Larring Y, Pishahang M, Tolchard J, Lind AM, Sunding MF, Stensrød RE, et al. Fabrication process parameters significantly affect the perovskite oxygen carriers materials (OCM) performance in chemical looping with oxygen uncoupling (CLOU). J. Therm. Anal. Calorim. 2020;140(2):577–89.
[13] Pishahang M, Larring Y, Sunding M, Jacobs M, Snijkers F. Performance of Perovskite-Type Oxides as Oxygen-Carrier Materials for Chemical Looping Combustion in the Presence of H_2S. Energy Technol. 2016;4(10):1305–16.
[14] Frick V, Rydén M, Leion H, Mattisson T, Lyngfelt A. Screening of supported and unsupported Mn-Si oxygen carriers for CLOU (chemical-looping with oxygen uncoupling). Energy 2015;93:544–54.
[15] Schmitz M, Linderholm C, Lyngfelt A. Chemical Looping combustion of sulphurous solid fuels using spray-dried calcium manganate particles as oxygen carrier. Energy Procedia. 2014;63:140–52.
[16] Shulman A, Cleverstam E, Mattisson T, Lyngfelt A. Manganese/Iron, Manganese/Nickel, and Manganese/Silicon Oxides Used in Chemical-Looping With Oxygen Uncoupling (CLOU) for Combustion of Methane. Energy Fuels 2009;23(10):5269–75.
[17] Mattisson T, Jing D, Lyngfelt A, Rydén M. Experimental investigation of binary and ternary combined manganese oxides for chemical-looping with oxygen uncoupling (CLOU). Fuel 2016;164:228–36.
[18] Abad A, Mendiara T, Izquierdo MT, de Diego LF, García-Labiano F, Gayán P, et al. Evaluation of the redox capability of manganese-titanium mixed oxides for thermochemical energy storage and chemical looping processes. Fuel Process. Technol 2021;211:106579. https://doi.org/10.1016/j.fuproc.2020.106579.
[19] Rydén M, Lyngfelt A, Mattisson T. Combined manganese/iron oxides as oxygen carrier for chemical looping combustion with oxygen uncoupling (CLOU) in a circulating fluidized bed reactor system. Energy Procedia 2011;4:341–8.
[20] Abad A, Adánez-Rubio I, Gayán P, García-Labiano F, de Diego L, Adánez J. Demonstration of chemical-looping with oxygen uncoupling (CLOU) process in a 1.5 kW_{th} continuously operating unit using a Cu-based oxygen-carrier. Int. J Greenh. Gas Control 2012;6:189–200.
[21] Adánez-Rubio I, Gayan P, Abad A, de Diego LF, García-Labiano F, Adánez J. Coal combustion by a spray granulated Cu-Mn mixed oxide for CLOU process. Appl. Energy 2017;208:561–70.
[22] Adánez-Rubio I, Izquierdo MT, Abad A, Gayan P, de Diego LF, Adánez J. Spray granulated Cu-Mn oxygen carrier for chemical looping with oxygen uncoupling (CLOU) process. Int. J. Greenh. Gas Control 2017;65:76–85.
[23] Adánez-Rubio I, Pérez-Astray A, Mendiara T, Izquierdo MT, Abad A, Gayán P, et al. Chemical looping combustion of biomass: CLOU experiments with a Cu-Mn mixed oxide. Fuel Process. Technol. 2018;172:179–86.
[24] Linderholm C, Mattisson T, Lyngfelt A. Long-term integrity testing of spray-dried particles in a 10-kW chemical-looping combustor using natural gas as fuel. Fuel 2009;88(11):2083–96.
[25] Success. Publishable Summary Report. EU 7th Framework Programme Collaborative Project 2017.
[26] G. Azimi H. Azimi M. Leion T. Rydén A. Mattisson Lyngfelt. Investigation of Different Mn–Fe Oxides as Oxygen Carrier for Chemical-Looping with Oxygen Uncoupling (CLOU) Energy Fuels 27 1 2013 367 377.
[27] Pérez-Vega R, Abad A, García-Labiano F, Gayán P, de Diego LF, Izquierdo MT, et al. Chemical Looping Combustion of gaseous and solid fuels with manganese-iron mixed oxide as oxygen carrier. Energy Convers. Manag. 2018;159:221–31.
[28] R. Pérez-Vega P. Gayán M.T. Izquierdo A. Abad F. García-Labiano L.F. de Diego et al. Development of Magnetic Mn-Fe Support materials for CLC applications 2018 Park City Utah, USA.
[29] J. Adánez L.F.D. Diego F. García-Labiano P. Gayán A. Abad M. Abián et al. Support and magnetic systems such as oxygen and CO2 carriers PCT/ES19/070122. CSIC (Ed.), 2019 Spain.
[30] Adánez-Rubio I, Bautista H, Izquierdo MT, Gayán P, Abad A, Adánez J. Development of a magnetic Cu-based oxygen carrier for the chemical looping with oxygen uncoupling (CLOU) process. Fuel Process. Technol. 2021;218:106836.
[31] ASTM. Standard test method for determination of attrition of FCC catalyst by air jets. ASTM D5757-11. Standard test method for determination of attrition of FCC catalyst by air jets 2006.
[32] Council IOO. http://www.internationaloliveoil.org. 2021.
[33] Fruit IND. http://www.nutfruit.org. 2021.
[34] Mei D, Linderholm C, Lyngfelt A. Performance of an oxy-polishing step in the 100 kW_{th} chemical looping combustion prototype. Chem. Eng. J. 2021;409:128202.